

Supplementary Information

Nanosized core-shell structured graphene-MnO₂ nanosheet arrays as stable electrodes for superior supercapacitors

He Nan Jia†, Jing Huang Lin†, Yu Lin Liu, Shu Lin Chen, Yi Fei Cai, Jun Lei Qi*, Ji

Cai Feng and Wei-Dong Fei*

State Key Laboratory of Advanced Welding and Joining, Harbin Institute of Technology, Harbin 150001, China

*Corresponding authors: Tel. /fax: 86-451-86418146;

†These authors contributed equally.

E-mail: jlqi@hit.edu.cn (J L Qi)

Calculations. The specific capacitance was calculated from CV curves the following equation by integrating discharge current I [1, 2],

$$C = \int IdV/2vm(orA)V,$$

where m is the weight of active materials (g), A is the area of the G@MnO₂ electrode (cm²), v is the scan rate (mV s⁻¹), and V is the sweep potential range of the CV curves (1 V). The power density (P , KW Kg⁻¹) and energy density (E , W h Kg⁻¹) were calculated from GCD curves [3],

$$E = \frac{0.5CV^2}{3.6}$$

$$P = \frac{3600E}{t}$$

where C is capacitance (F g⁻¹), V is the sweep potential range (1V), t is the discharge

time (s)

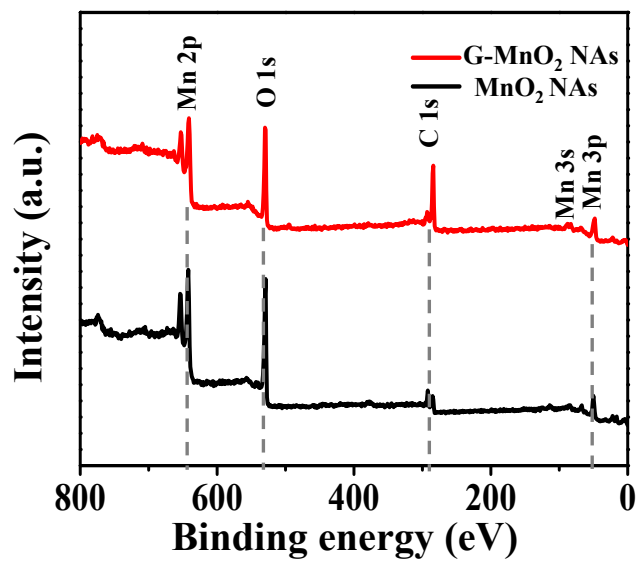


Figure S1. Survey XPS spectrum of MnO₂ NAs and G-MnO₂ NAs

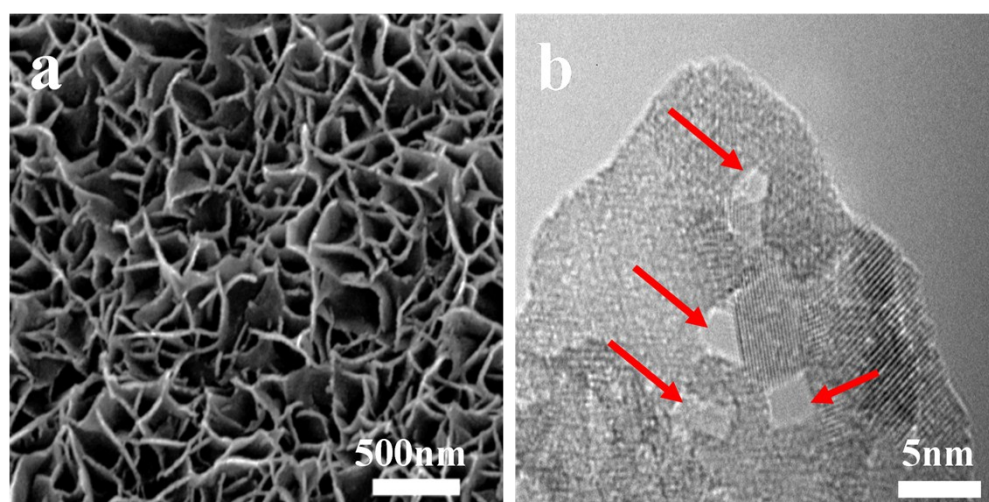


Figure S2. a) SEM image and b) TEM image of pristine MnO₂ nanosheets after argon plasma etching.

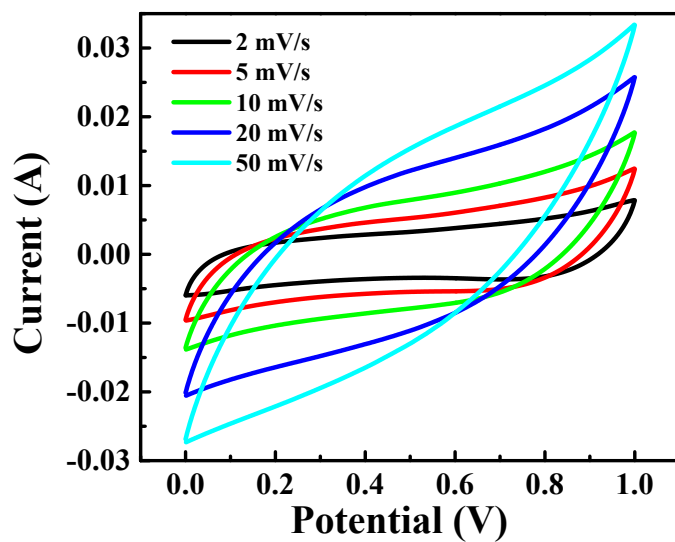


Figure S3. CV curves of MnO₂ NAs at different scan rates.

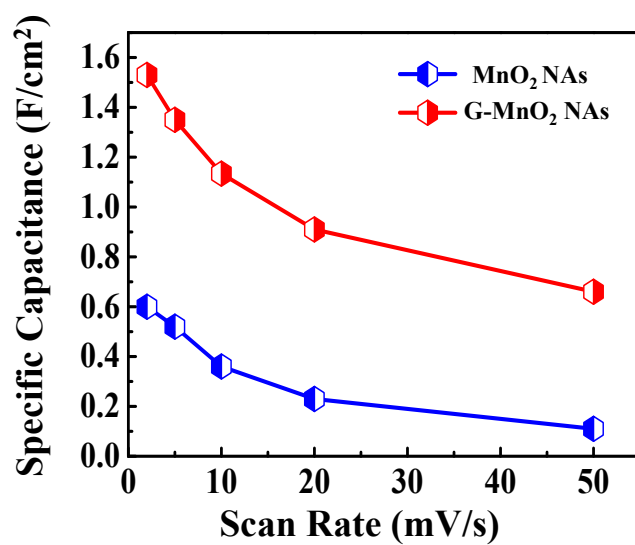


Figure S4. The areal specific capacitance for G-MnO₂ NAs and MnO₂ NAs as a function of the scan rate.

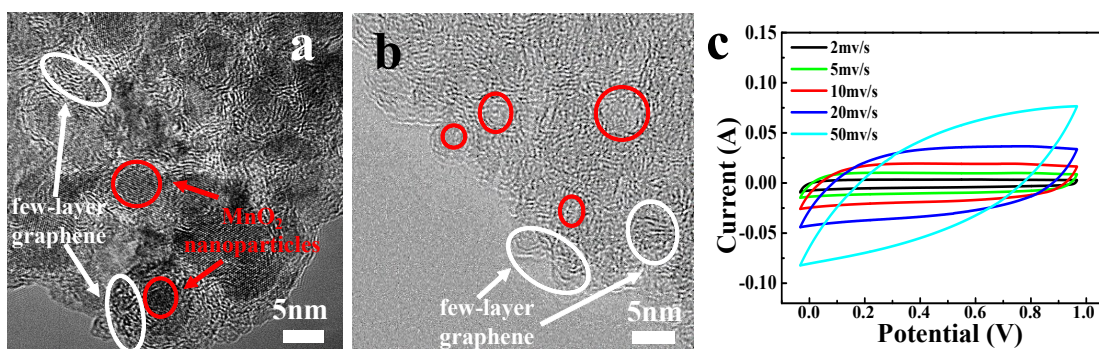


Figure S5. (a) TEM image of pristine G-MnO₂ NAs; (b) TEM image of G-MnO₂ NAs dissolved in 3M hydrochloric acid; (c) CV curves of porous graphene.

We dissolved the MnO₂ in G-MnO₂ NAs in 3M hydrochloric acid for 12 hours, then collected residuum (porous few-layer graphene) and dried it in a vacuum oven at 80 °C for 12 hours. As shown in Figure S5a, few-layer graphene shells in G-MnO₂ NAs act as a role of framework and encapsulate core MnO₂ nanoparticles. As shown in Figure S5b, few-layer graphene shells still maintain the shell structures well after corrosion. Furthermore, in the close observation of red cycles in Figure S5b, the disappearance of core materials (α -MnO₂ nanoparticles) suggests that few-layer graphene shells do not fully encapsulate nanoparticles. Next, the electrodes were prepared by homogeneously mixing these porous few-layer graphene (80 wt.%) and acetylene black (10 wt.%, Aladdin Chemistry) with polyvinylidene fluoride (10 wt.%) binder in N-methyl pyrrolidinone solvent. The slurry was then smeared onto a piece of nickel foam as current collector and dried in vacuum at 80°C for 12 h. The CV curves of porous graphene are shown in Figure S5c. It can be seen that the inferior area under the CV curve of porous few-layer graphene indicates that its capacitance (263 F g⁻¹ at scan rate of 2 mV s⁻¹) is extremely lower than that of the G-MnO₂ NAs (1176 F g⁻¹ at scan rate of 2 mV s⁻¹). As a result, it clear suggests that the contribution of MnO₂ nanoparticles which act as core materials is greater than few-layer graphene

shells during electrochemical process.

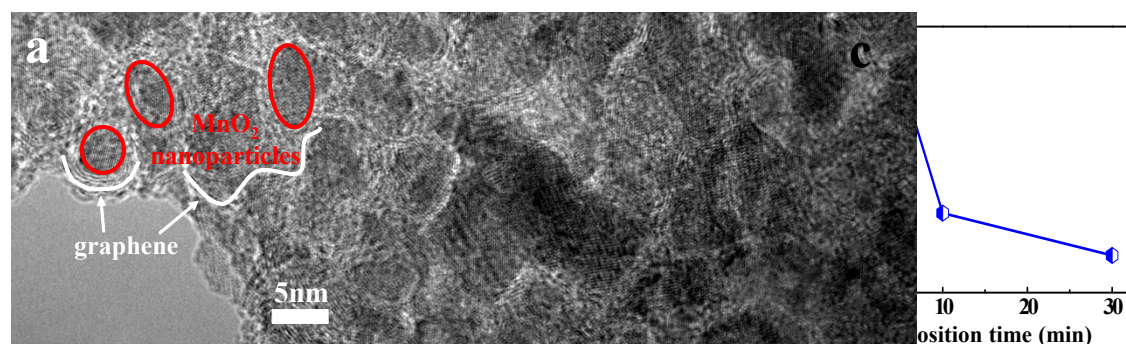


Figure S6. (a) TEM image of 30min@G-MnO₂ dissolved in 3M hydrochloric acid; (b) CV curves of 30min@G-MnO₂ at different scan rates; (c) Areal specific capacitance of MnO₂ with different deposition time (2 mV s⁻¹).

To further confirm the effect of few-layer graphene shells in G-MnO₂, we prolong the PECVD process to 30 min (30min@G-MnO₂) to fully encapsulate nanoparticles with few-layer graphene and supplement the CV curves for the obtained 30min@G-MnO₂. Figure S6a shows the TEM image of 30min@G-MnO₂, which was dissolved in 3M hydrochloric acid for 12 hours. Compared with Figure S5a and 5b, it remains some integrated core-shell structures, and the existence of MnO₂ nanoparticles illustrates the protective effect of fully-encapsulated few-layer graphene shells. And it also illustrates that prolonging deposition time can increase the content of few-layer graphene shells to fully encapsulate MnO₂ nanoparticles.

For further explaining the contribution of few-layer graphene, 30min@G-MnO₂ was directly used as the working electrode and the CV curve is shown in Figure S6b. However, the protective effect of few-layer graphene generates that it is hard to corrode MnO₂ nanoparticles, therefore the gravimetric specific capacitance which based on the weight of active materials is inaccurate to evaluate the role of graphene in 30min@G-MnO₂ during electrochemical measurement [4]. Thus, we select areal specific capacitance to better reflect the electrochemical contribution of graphene in

G-MnO₂ NAs. And the results show that areal specific capacitance of 30min@G-MnO₂ is 0.51 F cm⁻² at 2 mV s⁻¹ and 1.53 F cm⁻² of G-MnO₂ NAs (as shown in Figure S6c), which means that long-time PECVD deposition or fully-encapsulate MnO₂ nanoparticles with few-layer graphene would access to a downward trend of areal specific capacitance of G-MnO₂ NAs. Obviously, encapsulating superabundant few-layer graphene on MnO₂ nanoparticles has a negative effect on electrode performance G-MnO₂ NAs, mainly because of the sacrifice of contact area between MnO₂ and electrolyte [5, 6]. This also illustrates that few-layer graphene shells in G-MnO₂ NAs are conducive to conductivity and skeleton stability instead of improving areal specific capacitance [7], and nanoparticles afford the utilization of the pseudocapacity of MnO₂.

Table. S1. The specific capacitance and cycling stability of various MnO₂-based electrodes in the three-electrode system in references.

electrode materials	electrolyte	specific capacitance	capacitance retention	reference
α -MnO ₂ Nanowires@Ultrathin δ -MnO ₂ Nanosheets	6 M KOH	310.2 F·g ⁻¹ at 1A·g ⁻¹	98.1% after 10 000 cycles	8
Fe-doped MnO ₂ nanostructures	1 M Na ₂ SO ₄	283.4 F·g ⁻¹ at 1 A·g ⁻¹	100% after 2000 cycles	9
MnO ₂ hollow spheres/reduced graphene oxide	1 M Na ₂ SO ₄	471.5 F·g ⁻¹ at 0.8 A·g ⁻¹	92% after 1000 cycles	10
Ni/MnO ₂ -filter paper (FP)	1 M Na ₂ SO ₄	1160 mF·cm ⁻² at 5 mV·s ⁻¹	85.1% after 1000 cycles	11
Metal-free SWNT/carbon/MnO ₂ hybrid electrodes	0.5 M Na ₂ SO ₄	550 μ F·cm ⁻² at 20 mV·s ⁻¹	92.4% after 5000 cycles	12
MnO ₂ Nanosheet/ Carbon Fiber	1 M Na ₂ SO ₄	634.5 F·g ⁻¹ at 10mV s ⁻¹	~100% after 3000 cycles	13
MnO ₂ -RGO _{SILAR}	1 M Na ₂ SO ₄	987.5 F·g ⁻¹ at 2 A·g ⁻¹	~79% after 10000 cycles	14
α -MnO ₂ nanowires@Ni _{1-x} Mn _x O _y nanoflakes	0.5 M Na ₂ SO ₄	657 F·g ⁻¹ at 0.25 A·g ⁻¹	94.6% after 1000 cycles	15
Co ₂ AlO ₄ @MnO ₂ nanosheets	2 M KOH	915.1 F·g ⁻¹ at 2 A·g ⁻¹	96.1% after 3000 cycles	16
rGO/MnOx	[C ₂ MIm]BF ₄ electrolyte	202 F·g ⁻¹ at 1 mV·s ⁻¹	106% after 115000 cycles,	17
three-dimensional mesoporous MnO ₂ nanostructures	1 M Na ₂ SO ₄	322 F·g ⁻¹ at 1 A·g ⁻¹	90% after 8000 cycles	18
a vertically aligned Ni nanowire array- MnO ₂	0.5 M Na ₂ SO ₄	214 F·g ⁻¹ at 1 mV·s ⁻¹	103.7% after 20000 cycles	19
CuO@MnO ₂ core-shell nanostructures	1 M Na ₂ SO ₄	343.9 F·g ⁻¹ at 0.25 A·g ⁻¹	83.1% after 12 000 cycles	20
NiCo ₂ O ₄ @MnO ₂ nanosheet networks	1M KOH	913.6 F·g ⁻¹ at 0.5A/g	87.1% after 3000 cycles	21
MnO ₂ nanoflake@CNTs/Ni	1 M Na ₂ SO ₄	1072 F·g ⁻¹ at 1 A·g ⁻¹	-----	22
GF@PPy@MnO ₂	1 M Na ₂ SO ₄	600.0 F·g ⁻¹ at	92% after	22

		1 A·g ⁻¹	5000cycles	
MnO ₂ -MnO ₂ /nanographene/MECN	1 M Na ₂ SO ₄	894 F·g ⁻¹ at 1 mA·cm ⁻²	83% after 20 000 cycles	24
δ phase MnO ₂ on Ga-doped ZnO (GZO)	1 M Na ₂ SO ₄	1068 F·g ⁻¹ at 0.1 mA·cm ⁻²	76.8% after 13,000 cycles	25
Graphene-MnO ₂	1 M Na ₂ SO ₄	216 F·g ⁻¹ at 0.5 A·g ⁻¹	90% after 5000 cycles	26
Carbon Nanotube/MnO ₂	1 M Na ₂ SO ₄	300 F·g ⁻¹ at 0.1 A·g ⁻¹	75% after 1600 cycles	27
G-MnO ₂ NAs	1M Na ₂ SO ₄	1176 F·g ⁻¹ at 2 mV·s ⁻¹	98.1% after 10000 cycles	This work

Reference:

- [1] E. Eustache, C. Douard, R. Retoux, C. Lethien and T. Brousse, *Adv. Energy Mater.*, 2015, **5**,18.
- [2] Y. Huang, Y. Li, Z. Hu, G. Wei, J. Guo and J. Liu, *J. Mater. Chem. A*, 2013, **1**, 9809.
- [3] Z. Li, Y. An, Z. Hu, N. An and Y. Zhang, *J. Mater. Chem. A*, 2016, **4**, 10618.
- [4] Z. Zhang, F. Xiao, L. Qian, J. Xiao, S. Wang and Y. Liu, *Adv. Energy Mater.*, 2014, **4**, 1400064.
- [5] R. Miller, R. A. Outlaw and B. C. Holloway, *Science*, 2010, **329**, 1637–1639.
- [6] G. Hahm, R. A. M. Reddy, D. P. Cole, M. Rivera, J. A. Vento, J. Nam, H. Y. Jung, Y. L. Kim, N. T. Narayanan, D. P. Hashim, C. Galande, Y. J. Jung, M. Bundy, S. Karna, P. M. Ajayan and R. Vajtai, *Nano Lett.*, 2012, **12**, 5616–5621.
- [7] M. F. El-Kady, M. Ihns, M. Li, J. Y. Hwang, M. F. Mousavi, L. Chaney, A. T. Lech and R. B. Kaner, *Proceedings of the National Academy of Sciences*, 2015, **112**, 4233-4238.
- [8] Z. Ma, G. Shao, Y. Fan, G. Wang, J. Song and D. Shen, *ACS Appl. Mater. Inter.*, 2016, **8**, 9050-9058.

- [9] Z. Wang, F. Wang, Y. Li, J. Hu, Y. Lu and M. Xu, *Nanoscale*, 2016, **8**, 7309-7317.
- [10] M. Lin, B. Chen, X. Wu, J. Qian, L. Fei, W. Lu, L. W. Chan and J. Yuan, *Nanoscale*, 2016, **8**, 1854-1860.
- [11] L. Zhang, P. Zhu, F. Zhou, W. Zeng, H. Su, G. Li, J. Gao, R. Sun and C. Wong, *ACS Nano*, 2016, **10**, 1273-1282.
- [12] L. Sun, X. Wang, K. Zhang, J. Zou and Q. Zhang, *Nano Energy*, 2016, **22**, 11-18.
- [13] N. Yu, H. Yin, W. Zhang, Y. Liu, Z. Tang and M. Zhu, *Adv. Energy Mater.*, 2016, **6**, 1501458.
- [14] M. Jana, S. Saha, P. Samanta, N. C. Murmu, N. H. Kim, T. Kuila and J. H. Lee, *J. Power Sources*, 2017, **340**, 380-392.
- [15] H. Y. Wang, F. X. Xiao, L. Yu, B. Liu and X. W. D. Lou, *Small*, 2014, **10**, 3181-3186.
- [16] F. Li, H. Chen, X. Y. Liu, S. J. Zhu, J. Q. Jia, C. H. Xu, F. Dong, Z. Q. Wen and Y. X. Zhang, *J. Mater. Chem. A*, 2016, **4**, 2096-2104.
- [17] Y. Wang, W. Lai, N. Wang, Z. Jiang, X. Wang, P. Zou, Z. Lin, H. J. Fan, F. Kang, C. Wong and C. Yang, *Energy Environ. Sci.*, 2017, DOI: 10.1039/c6ee03773a.
- [18] S. Bag and C. R. Raj, *J. Mater. Chem. A*, 2016, **4**, 587-595.
- [19] C. Xu, Z. Li, C. Yang, P. Zou, B. Xie, Z. Lin, Z. Zhang, B. Li, F. Kang and C. P. Wong, *Adv. Mater.*, 2016, **28**, 4105.
- [20] H. Chen, M. Zhou, T. Wang, F. Li and Y. X. Zhang, *J. Mater. Chem. A*, 2016, **4**, 10786-10793.
- [21] Y. Zhang, B. Wang, F. Liu, J. Cheng, X. W. Zhang and L. Zhang, *Nano Energy*, 2016, **27**, 627-637.
- [22] P. Sun, H. Yi, T. Peng, Y. Jing, R. Wang, H. Wang and X. Wang, *J. Power Sources*, 2017, **341**, 27-35.

- [23] T. Qin, B. Liu, Y. Wen, Z. Wang, X. Jiang, Z. Wan, S. Peng, G. Cao and D. He, *J. Mater. Chem. A*, 2016, **4**, 9196-9203.
- [24] D. Wu, S. Xu, C. Zhang, Y. Zhu, D. Xiong, R. Huang, R. Qi, L. Wang and P. K. Chu, *J. Mater. Chem. A*, 2016, **4**, 11317-11329.
- [25] L. Yang, S. Cheng, J. Wang, X. Ji, Y. Jiang, M. Yao, P. Wu, M. Wang, J. Zhou and M. Liu, *Nano Energy*, 2016, **30**, 293-302.
- [26] L. Sheng, L. Jiang, T. Wei and Z. Fan, *Small*, 2016, **12**, 5217-5227.
- [27] H. Chen, S. Zeng, M. Chen, Y. Zhang, L. Zheng and Q. Li, *Small*, 2016, **12**, 2035-2045.